ELSEVIER

UV patterning of polyimide: differentiation and characterization of surface chemistry and structure

J.A. Blach-Watson[a,b,*], G.S. Watson[a], C.L. Brown[a,b], S. Myhra[a]

[a]*School of Science, Griffith University, Kessels Road, Nathan, Brisbane, Qld 4111, Australia*
[b]*CRC for MicroTechnology, Level 5, 60 William Street, Hawthorn, Vic. 3122, Australia*

Abstract

Polyimides are representatives of high-performance polymers. One member of the family (PI-2730 series) has found application as a photodefinable negative resist, allowing the surface chemistry to be altered through UV exposure. The evolution in lateral differentiation arising from masking and subsequent exposure has been investigated. Analysis showed that exposure resulted in increasing hydrophilicity, as well as shrinkage of the exposed areas. A particular focus of the study has been on the effect of lateral chemical differentiation on selective adsorption of functionalised beads, and on arrays of precipitate structures.
© 2004 Elsevier B.V. All rights reserved.

1. Introduction

Surface structure and surface chemistry play leading roles in polymer functionality. Any changes to these, e.g. due to deposition of energy arising from UV irradiation, can alter the chemistry as well as mechanical properties of the surface and near-surface layers [1]. Polyimides are representatives of high-performance polymers which possess distinct attributes, such as good thermal stability (>500 °C), exceptional toughness and mechanical strength, and chemical resistance to many reactive industrial fluids. The PI-2730 series photodefinable negative resist is used extensively in the electronics industry. Given that

the surface chemistry can be altered by UV irradiation, they may also have potential as substrates for bioactive/selective sensor arrays. This study describes the physicochemical effects of surface patterning by UV irradiation.

2. Experimental details

2.1. Polyimide films and surface patterning

The polyimide precursor was supplied by DuPont™ (PI-2737). The films were spun-coated onto Si wafer substrates, and cured at 350 °C for 1 h under a nitrogen atmosphere. The resulting surface topography was characterized by AFM in the contact mode. The thicknesses of some films were measured from the step height from the Si substrate (following

---

* Corresponding author. Tel.: +61 7 3875 7531;
fax: +61 7 3875 7656.
E-mail address: j.blach@griffith.edu.au (J.A. Blach-Watson).

development and removal of unirradiated material) to be 600 ± 100 nm. The RMS surface roughness was determined by AFM imaging to be ca. 10 nm for a typical area of $10 \times 10 \ \mu m^2$.

The patterning consisted of masking and irradiation, without any additional processing. The exposure was carried out with a Super Spot MK III High Intensity Ultraviolet Light Spot Curing System. The system can deliver a maximum intensity of 20 W/cm^2 in UVA and 25 W/cm^2 in UV–vis. The surfaces were masked by square copper (40 μm pitch) or stainless steel (80 μm pitch) TEM grids. The duration of exposure ranged from 90 to 540 s, at 90 s increments. The temperature rise of the specimen was limited to a maximum 85 °C by placing the specimen a distance of 0.5 cm from the aperture of the source.

2.2. AFM analysis and other methodology

The analysis was carried out with two instruments: a TopoMetrix TMX 2000 Explorer system, with $130 \times 130 \ \mu m^2$ air and liquid scanners, with a *z*-range of 9.7 μm, and a JEOL JSPM-4200, with 25×25 and $85 \times 85 \ \mu m^2$ scanners, with a *z*-range of ca. 3 μm. Data were obtained in the contact imaging, force versus distance (*F–d*) and lateral force modes of operation. The lever-imposed loading force depended on the choice of lever stiffness, and ranged from 12 to 55 nN during topographic and friction loop analyses. Each *F–d* curve consisted of 600 data points; the curves were taken at random locations within a field of view, in order to average out possible topographical effects on the data. Some experiments were carried out under air-ambient temperatures and relative humidity (21–25 °C and 50–60%).

Probes were obtained from Ultrasharp NT-MDT. A beam-shaped variety was chosen in order to facilitate interpretation of lateral force data. The normal spring constants, k_N, were determined by the resonance method [2], and ranged from 0.023 to 0.13 N/m.

Nominally 'bare' and Au-coated etched Si tips were used during the experiments. As-received probes are generally stored on a silicone pad, and an unintended consequence is that the probes will become coated by poly(dimethylsiloxane) (PDMS), which forms a thin hydrophobic layer [3]. Thus the as-received probes will present hydrophobic surface chemistry. Chemical cleaning in 'piranha' solution is required to remove

this film [3], and thus produce a hydrophilic Si-oxide or metallic Au surface layer. In order to prepare a hydrophilic tip surface at near-neutral pH, two gold-coated tips were functionalised in a EtOH solution with 1 mM 11-mercaptoundecanoic acid ($HS(CH_2)_{11}CO_2H$) for ca. 12 h.

Deposition onto the polymer surface of colloidal beads in the 5 μm size range was used as a diagnostic tool for exploration of laterally differentiated surface chemistry. Hydrophilic silica (S-series, Bangs Laboratories) and silica beads with hydrophobic silane-coupled CH_3-terminated alkyl chains (Polysciences, Inc.) were used for that purpose.

3. Results and discussion

3.1. Surface patterning

Shrinkage was found to be an unintended by-product of UV exposure; it was linearly dependent on exposure time over a range of 20–100 nm for exposure times up to 600 s. Similar observations have been made for other polymers [1]. The effect is presumably due to either loss of material and/or densification arising from the exposure. A topographical image and line profile for an exposure of 540 s are shown in Fig. 1a and b.

3.2. Surface chemistry

F–d analysis is a rich source of information about the chemical and mechanical surface properties at the tip-to-surface point of contact, e.g. Ref. [4]. In the present context the mode provides the following information:

- The snap-on feature in the approach curve, in air, will occur at the point where the tip 'senses' the short-range interaction with the adsorbed aqueous phase. The size is a measure of the thickness of the compressible/penetrable surface layer. Polyimide is effectively incompressible and the snap-on distance in air is a measure of thickness of adsorbed water.
- The snap-on feature is usually much less prominent when *F–d* analysis is undertaken under water. The capillary force is then removed from the system. However, a smaller snap-on will be evident due to
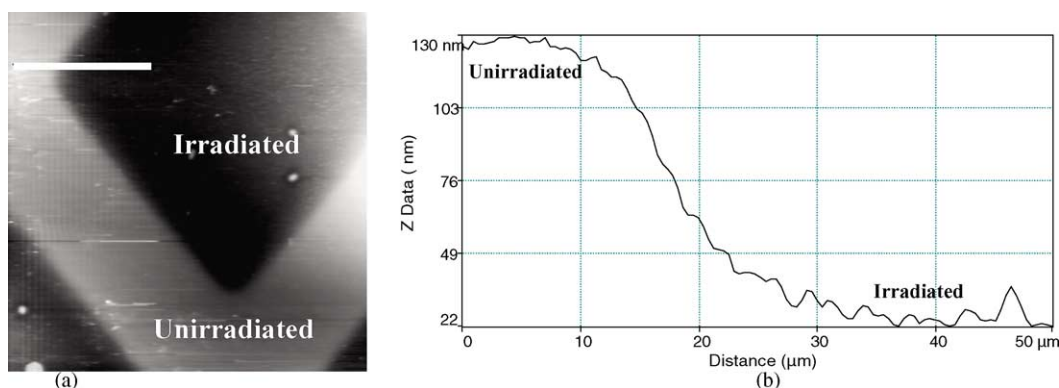
Fig. 1. Topography (a) and line profile (b) for a surface exposed for 540 s. The shrinkage is apparent.

hydrophobic/hydrophilic effects, and due to short-range interaction at the tip-to-polymer interface.

- The lift-off feature in the retract curve is conventionally taken as a measure of tip-to-surface adhesion, F_{adh}. In the present context the contributions to adhesion can be written as

$$F_{adh} = F_{meniscus} + F_{hyd} + F_{TS} \qquad (1)$$

where $F_{meniscus}$ dominates in air (in the range 20–200 nN), F_{hyd} arises from hydrophobic/hydrophilic interactions (<5 nN), while F_{TS} is the tip-to-solid interaction (<1 nN).

- Non-linearities in the approach and/or retract curve, when the tip is in contact, will be due to relaxation/compression at the point of contact arising from dependence on force loading. Linearity is consistent with polyimide being incompressible (the bulk elastic modulus is 4.7 GPa) in comparison with the lever with $k_N < 0.13$ N/m.

Fig. 2 shows diagrammatically the adhesive and frictional trends for various combinations of tips, media, and surfaces. The respective strengths of adhesion for irradiated polyimide and Si were ca. 12 and 15 nN, with Si exhibiting the higher adhesion (the Si substrate was used as an internal calibration standard). A Si-substrate exposed to air will be terminated by a thin native oxide layer, therefore clean Si-oxide is hydrophilic.

Snap-on features and adhesion in air will be dominated by a capillary force, thus masking interactions that are direct consequences of surface chemistry, e.g. hydrophobicity/hydrophilicity. If tip geometry and

chemistry remain invariant, then the greater meniscus force for a UV-exposed surface, in comparison with an as-received surface, must be due to a greater thickness of adsorbed moisture. Likewise, the greater thickness of adsorbed moisture will manifest itself as a larger snap-on distance. A hydrophilic tip will exhibit greater snap-on distances, and greater capillary attraction, in comparison with a hydrophobic tip
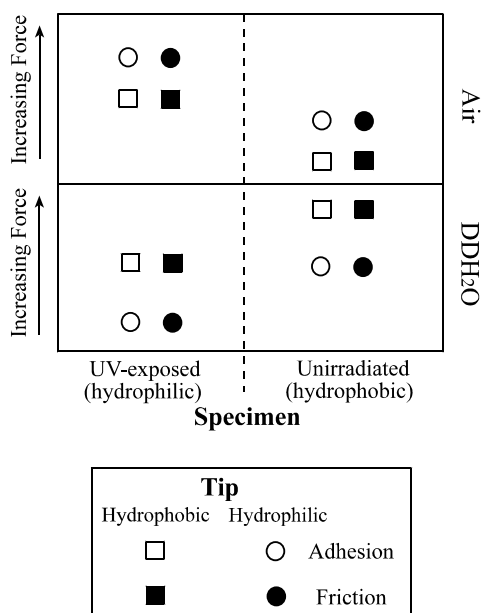

Fig. 2. Diagrammatic representation of adhesive and frictional trends with respect to environment (air and DDH$_2$O), using both hydrophobic and hydrophilic probes on UV-exposed and as-received surfaces. Relative magnitudes are indicated by the arrows on the left, with zero at the horizontal centre line.
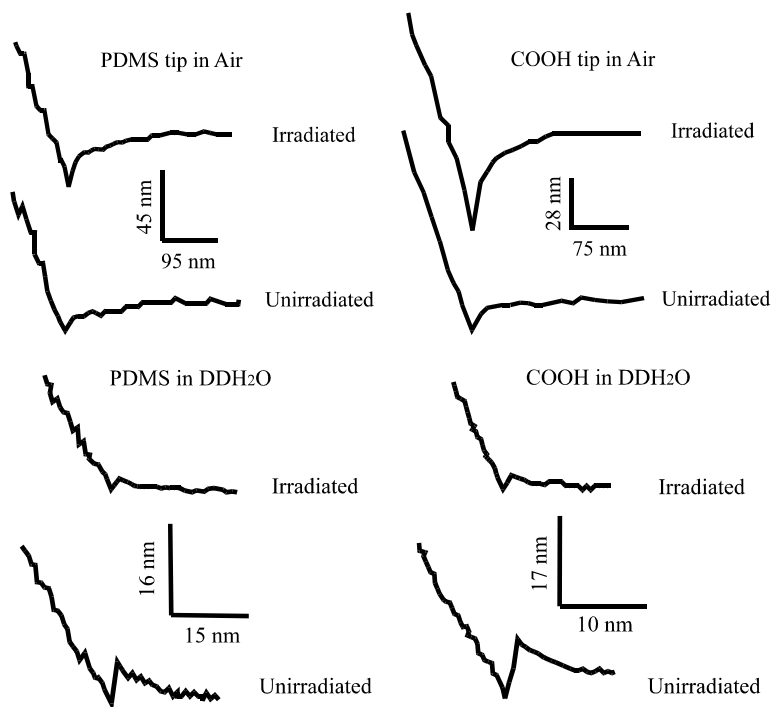
Fig. 3. Representative approach curves showing dependence of snap-on distances on surface chemistry of tip (PDMS and COOH functionalisation), surface (UV-exposed vs. as-received), and ambient (air (top) and DDH$_2$O (bottom)).

(Fig. 3, top). When the experiments are performed in DDH$_2$O (MilliQ water), capillary interaction is eliminated, and the interaction is thus represented by the chemistries of the two surfaces in contact (Fig. 3, bottom).

The strength of the adhesive interaction will depend on the degree of hydrophobicity/hydrophilicity on both the tip and surface. When contact is made between tip and surface, where both are hydrophilic, then the adhesive force will be lower than that when both surfaces are hydrophobic [5]. Adhesion will also depend on the pH of the medium (due to electrostatic interactions), on van der Waals interactions, and on steric/topographic factors. A pH above the iso-electric point (ca. pH 5) will cause deprotonation of COOH groups either on the tip or on the surface, raising the repulsive electrostatic interactions and consequently lowering adhesion [6,7]. In the present case the pH was ca. 5.8.

The thickness of the adsorbed layer will depend on ambient humidity and on surface chemistry of the substrate [8]. Even though gold tips coated by PDMS

are hydrophobic, the interaction with a hydrophobic surface in an air environment will also be attractive, but the strength of attraction will be less than that for two interacting hydrophilic surfaces.

The lateral force mode (LFM) will reveal image contrast arising from laterally differentiated surface chemistry that will manifest itself as a variable frictional force. The relationship between a normal force and lateral in-plane force components sensed by a tip in sliding contact can be described by

$$F_L = \mu F_N^* \tag{2}$$

where $F_N^* = F_N + F_{adh}$ (the sum of lever-imposed force and adhesive interactions), and μ is the coefficient of 'friction'. The expression is of reasonable validity in the multi-asperity regime. The linear dependence implies that the lateral force will scale with strength of adhesion, for constant lever-imposed normal force. LFM analysis of UV-patterned surfaces showed higher friction on the irradiated regions in air (Fig. 4a). That result is consistent with that surface being hydrophilic, and is in agreement with the
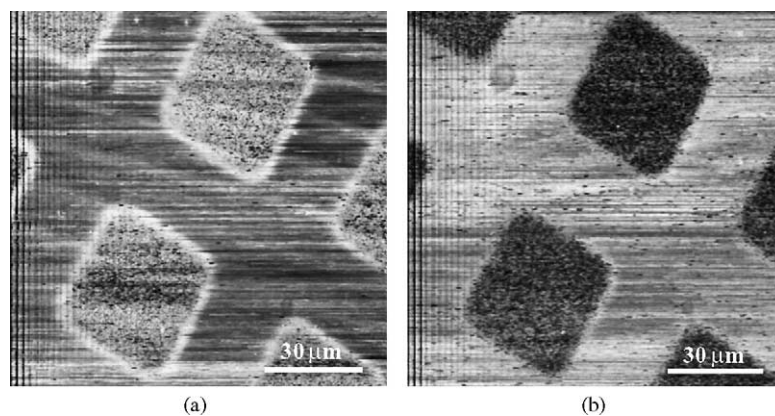
Fig. 4. Lateral force maps taken in air (a) and in DDH$_2$O (b). The brighter contrast represents higher friction.

observed higher adhesion. The capillary force is the dominant adhesive interaction during analysis in air, and will produce contrast that is proportional to the thickness of the layer of adsorbed moisture. Thus the more hydrophilic regions will have brighter lateral contrast. When the analysis is carried out under water, the capillary force is eliminated, and the contrast will reverse (Fig. 4b). A comparison of outcome of LFM
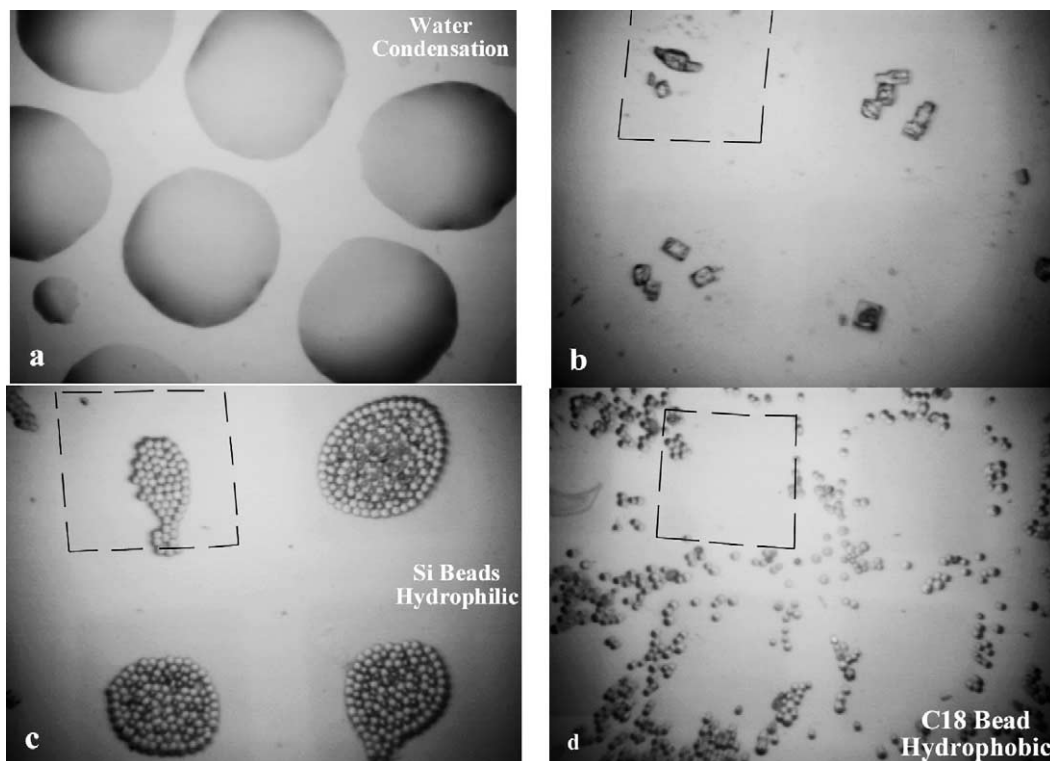

Fig. 5. Optical images of (a) adsorbed moisture, (b) salt precipitation, (c) hydrophilic beads, and (d) hydrophobic beads. The outlined squares show UV exposure pattern.

analysis for a hydrophobic PDMS-coated tip or a hydrophilic COOH-terminated tip shows that in DDH$_2$O the adhesion, and thus lateral force, is lowest when a hydrophilic tip is interacting with a hydrophilic surface. Those results are consistent with observations on related systems [9,10].

3.3. Spatially resolved adsorption

The implications of laterally differentiated surface chemistry were explored in a series of experiments. The optical images in Fig. 5a and b illustrate an ordered array arising from condensation of water vapour on hydrophilic regions, while spatially resolved precipitate decoration is shown to result from evaporation of droplets containing salt in solution. Exposure of the patterned surfaces to hydrophilic and hydrophobic beads in solution lead to inclusion and exclusion, respectively, from the hydrophilic regions (Fig. 5c and d). The effect arises from the beads being trapped in solution in an ordered array of droplets. The hydrophilic beads will simply plate out onto the irradiated regions. The hydrophobic beads, on the other hand, will be expelled from those regions during evaporation, and will preferentially attach to the hydrophobic regions. Functionalised beads of different chemistries can be contained to specific regions determined by the irradiation surface maps.

4. Conclusions

Radiation patterning has proven to be a reliable and convenient tool for producing laterally differentiated surface chemistries on photosensitive polymer resists. Imaging of irradiated surfaces revealed shrinkage and also strong evidence for a change in chemistry from hydrophobic to hydrophilic. Irradiation was found to cause an increase in both adhesion and friction, measured in air using hydrophobic and hydrophilic probes, which arises from an increase in hydrophilicity and thus greater capillary interaction. In DDH$_2$O, the capillary force was eliminated revealing the dominant attractive interaction associated with hydrophobicity. UV patterning will promote spatially resolved aqueous condensation, and thus offer preferred sites for adsorption of species from solution.

References

[1] J.A. Blach, G.S. Watson, W.K. Busfield, S. Myhra, Polym. Int. 51 (2002) 12.
[2] J.P. Cleveland, S. Manne, D. Bocek, P.K. Hansma, Rev. Sci. Instrum. 64 (1993) 403.
[3] Y.-S. Lo, N.D. Huefner, W.S. Chan, P. Dryden, B. Hagenhoff, T.P. Beebe, Langmuir 15 (1999) 6522.
[4] N.A. Burnham, R.J. Colton, H.M. Pollock, Nanotechnology 4 (1993) 64.
[5] S.K. Sinniah, A.B. Steel, C.J. Miller, J.E. Reutt-Robey, J. Am. Chem. Soc. 118 (1996) 8925.
[6] E.W. van der Vegte, G. Hadziioannou, J. Phys. Chem. B 101 (1997) 9563.
[7] D.V. Vezenov, A. Noy, L.F. Rozsnyai, C.M. Lieber, J. Am. Chem. Soc. 119 (1997) 2006.
[8] X. Xiao, L. Qian, Langmuir 16 (2000) 8153.
[9] E.W. van der Vegte, G. Hadziioannou, Langmuir 13 (1997) 4357.
[10] M.P.L. Werts, E.W. van der Vegte, G. Hadziioannou, Langmuir 13 (1997) 4939.